RSC Advances

PAPER

View Article Online
View Journal | View Issue

Cite this: *RSC Adv.*, 2020, **10**, 41229

Efficient *N*-formylation of primary aromatic amines using novel solid acid magnetic nanocatalyst†

Jitendra Kumar Yadav,[a] Priyanka Yadav,[b] Satish K. Awasthi[*b] and Alka Agarwal[*a]

Received 31st August 2020
Accepted 29th October 2020

DOI: 10.1039/d0ra07476d

rsc.li/rsc-advances

Sulfonic acid functionalized over biguanidine fabricated silica-coated heterogeneous magnetic nanoparticles (NP@SO_3H) have been synthesized, well characterized and explored for the first time, as an efficient and recyclable catalyst for *N*-formylation of primary amines under mild reaction conditions. Exploiting the magnetic nature of Fe_3O_4, the prepared catalyst was readily recovered from the reaction mixture *via* an external magnet. The catalyst can be reused for up to six cycles without any substantial loss of catalytic activity. The cost effectiveness, simple methodology, wide substrate tolerance, excellent yield and easy work-up are the additional advantages of present catalytic system.

Introduction

Formamides are an important class of organic compounds which possess a very wide range of applications in synthetic chemistry such as Vilsmeier formylation reactions[1,2] and as polar solvents in various organic reactions and medicinal chemistry.[3] By statistical figures, it is found that nearly one-fourth of all pharmaceuticals drugs such as paracetamol, formoterol, captopril and chloramphenicol have amide bonds (Fig. 1).

All these drugs are clinically used for the treatment of fever, lung diseases, hypertension and bacterial diseases respectively.[4,5] Formamides are also extensively used as Lewis base catalysts in allylation,[6] and hydrosilation[7] of carbonyl compounds. Moreover, it is also well documented that the formyl group is the best amino-protecting group in peptide synthesis,[8] and they are also important precursors in the preparation of formamidines, isocyanides, and heterocycles.[9] Generally, the *N*-formylation reaction of amines are proceeded by various formylating reagents such as formic acid-DCC,[10] formic acid-EDCL,[11] formic acid in toluene,[12] *N*,*N*-dimethylformamide (DMF),[13] acetic formic anhydride,[14] ammonium formate,[15] chloral[16] trialkyl orthoformates, enol formates, cyanomethyl formate,[17] and cyanide[18] *etc.*

Since then, many reports have appeared in the literature for the formylation of amines under the influence of several catalysts, various solvents and under reaction conditions. The numerous catalysts including their methodology and biological application have also been reported till date such as copper, Fe(III),[19], $[Pd(OAc)_2]$,[20] $ZnCl_2$ and Lewis acids,[21] ZnO,[22] carbon nanotube–gold nanohybrid (Au–CNT),[23] indium,[24] nanocerium oxide,[25] K_3PO_4,[26] heteropolyanion-based ionic liquids (HPAILS),[27] oaryloxide–*N*-heterocyclic carbene ruthenium(II) ([Ru–NHC] complex),[28] molybdate sulfuric acid,[29] $H_2SO_4SiO_2$,[30] sulfated tungstate catalyst,[31] and many others. Most of these methodologies have some drawbacks such as harsh reaction conditions, low yield, high temperature, long reaction time and expensive reagents. Moreover, these catalysts are either toxic or less accessible, thermally unstable, poor functional group or formation of side products, applicable only to aromatic amines and the preparation and use of these reagents require strictly anhydrous conditions.[32,33] Thus, there is still some scope to improve and develop newer, simple and an efficient reagent to overcome or minimize these drawbacks. Therefore, the development of a new methodology for *N*-formylation is still desirable.

Our research group is working on designing inorganic–organic hybrid magnetic nanocatalyst for catalytic activity. In

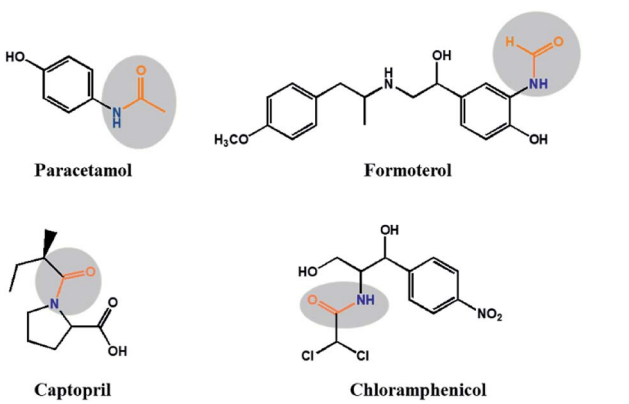

Fig. 1 Some of market drugs containing amide functional group.

[a]*Department of Medicinal Chemistry, Institute of Medical Sciences, Banaras Hindu University, Varanasi, UP, India. E-mail: agarwal.dralka@gmail.com*

[b]*Chemical Biology Laboratory, Department of Chemistry, University of Delhi, Delhi, Delhi-110007, India. E-mail: satishpna@gmail.com*

† Electronic supplementary information (ESI) available: ^1H NMR and ^{13}C NMR chemical shift values; ^1H NMR and ^{13}C NMR spectra, mass spectra of all the synthesized compounds, FT-IR and powder XRD of reused catalyst (NP@SO_3H) after 6 serial runs. See DOI: 10.1039/d0ra07476d

continuation of our research work,[34] we are here reporting an efficient, mild and green method for the *N*-formylation of amines with formic acid using NP@SO_3H as a newer catalyst comprising of sulfonic acid over biguanidine moieties.

Biguanides are widely used as a antihyperglycemic agents that suppress hepatic glucose production, increase peripheral glucose uptake, and moderately reduce LDL cholesterol and triglyceride levels. For example metformin is widely used to treat diabetes, proguanil and chlorproguanil are used as anti-malarial drugs. As compared to a guanidine biguanide has a higher ability to bind metals because of the two imine-like functions and thus acts as a bidentate ligand (Fig. 2).[35,36]

The regular acid catalysts includes mineral acids *viz.* H_2SO_4, HCl, HF and other organic acids like *p*-toluene sulfonic acid, leading to severe disadvantages like corrosion, toxicity, tedious separation of catalysts from homogeneous reaction mixtures and urgency of neutralization of waste streams. Among them sulfonic acid is corrosive liquid acid having high activity, is efficiently used to synthesize different organic compounds. However, being corrosive in nature, it is hazardous and harmful for environment as well as public health. It is deadly if inhaled or swallowed and cause eyes and skin burn. It reacts readily with water generating toxic liquid, hydrochloric acid (HCl) and sulfur dioxide (SO_2). Also, the adversity of its separation from reaction medium limits its applicability in pharmaceutics and industries.[37–42] Thus, we have designed and synthesized heterogeneous sulfonic acid fabricated over biguanidine functionalized silica coated iron oxide nanoparticles to overcome the draw backs and make it suitable and safer use of this efficient acid heterogeneous catalyst.

To the best of our knowledge, this is the first report on catalytic performance of NP@SO_3H for *N*-formylation of amines. Moreover, the newer synthesized catalyst is expected to show very unique and efficient catalytic performance owing to heterogeneous as well as presence of large number of catalytic sites.[43] This newer developed nanocatalyst also has an advantage of being magnetically recoverable from reaction mixtures using external magnetic force, thereby eliminating the requirement of catalyst filtration or centrifugation after completion of the reaction as in the case of other solid support materials. Hence, the major advantage of the present magnetic nanocatalyst, apart from their relative non-toxicity, high air and thermal stability, chemical stability, easy separation from reaction medium, facile recyclability, non-hygroscopic nature, and excellent catalytic performance. We further believe that the present nanocatalyst can be surface-modified so as to increase its catalytic activity as well as selectivity towards different organic transformations.

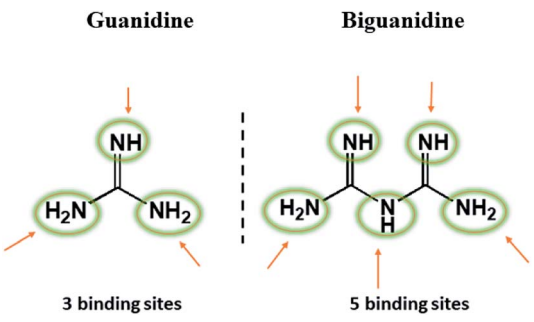

Fig. 2 Comparison of binding sites for guanidine and biguanidine group.

Experimental

Materials

Ferric and ferrous sulfate were procured from Sisco Research Laboratory (SRL). Tetra-ethyl orthosilicate (TEOS) and APTES were obtained from Sigma-Aldrich. All analytical grade chemicals used in the experiment were purchased from Merck and Alfa-Aesar and used without any further purification. Double-distilled water was used throughout the experiment.

Instrumentation

Fourier transform infrared (FT-IR) spectra were recorded using KBr pellet method that was operative in the range of 400–4000 cm^{-1} at room temperature on a PerkinElmer Spectrum RXI-Mid IR spectrometer. The information about the size, shape and morphology of the nanocatalyst was obtained through transmission electron microscopy (TEM), performed on a 200 kV, TECNAI 20G2 FEI and scanning electron microscopy measurement (SEM) using a ESEM QUANTA-200. Energy-Dispersive X-ray (EDX) studies (equipped with the SEM instrument) were performed for elemental analysis of NP@SO_3H. The mass and nuclear magnetic resonance (^1H and ^{13}C) spectra of the *N*-formylation product were recorded on a HR-MS and JEOL GS-400 model at 400 MHz and 100 MHz respectively.

Catalyst preparation

Preparation of the amine functionalized magnetic Fe_3O_4 nanoparticles (ASMNPs). The amine functionalized silica coated nanoparticles (ASMNPs) were prepared as per our previous report.[34] Briefly magnetic nanoparticles (MNPs) were prepared by co-precipitation method. Then these MNPs were coated with dense layer of silica by sol–gel approach to avoid leaching of iron from the core and obtain silica coated magnetic nanoparticles (SMNPs). Afterwards, SMNPs were functionalized with APTES to obtain ASMNPs.

Incorporation of biguanidine group to Fe_3O_4@SiO_2–NH_2 magnetic nanoparticles. In order to extend the number of catalytic sites over the surface of nanoparticles, biguanidine functionality was introduced on ASMNPs. To achieve it, ASMNPs (3 g) and dicynoguanidine (750 mg) were suspended in 100 mL of absolute ethanol. The reaction mixture was refluxed at 60 °C for 12 h. The resulted biguanidine group containing magnetic nanoparticles (NP) were separated using external magnet and washed thoroughly with deionized water (2 × 5 mL) and ethanol (2 × 5 mL) and dried in vacuum oven for 6 h.

Incorporation of SO_3H group to Fe_3O_4@SiO_2–NH_2 containing biguanidine group (NPs). Biguanidine functionalized silica coated magnetic nanoparticles (NPs) (3 g) were dispersed in dry CH_2Cl_2 (150 mL) using ultrasonic bath for 30 min. Subsequently, 12 mL chlorosulfuric acid ($ClSO_3H$) was added

dropwise with constant stirring over a period of 45 min in ice both. Hydrogen chloride (HCl) gas evolved from the mixture immediately. The prepared sulfonated nanoparticles ($NP@SO_3H$) were separated by magnetic decantation and washed with dry CH_2Cl_2 (5 × 4 mL) to remove the unattached substrates and dried well under vacuum oven.

Procedure for *N*-formylation using $NP@SO_3H$ as a catalyst. A mixture of formic acid (4 mmol), aromatic amine (1 mmol) and $NP@SO_3H$ (10 mg) taken in oven-dried round bottom flask, were dispersed in absolute ethanol (2 mL). The reaction mixture was allowed to stir at room temperature and progress of the reaction was monitored by TLC. After the completion of the reaction, the catalyst was separated using external magnet and washed thoroughly with absolute ethanol. The remaining ethanol in the round bottom flask was evaporated using rotavapour and that crude product was purified by recrystallization using *n*-hexane/ethyl acetate or by short column chromatography on silica gel to obtain pure product. The purified products were characterized by using HR-MS, ^1H and ^{13}C NMR.

Results and discussion

The stepwise synthesis of magnetic nanoparticles $NP@SO_3H$ is shown in Scheme 1.

Firstly, MNPs were prepared using co-precipitation method by mixing two different salts of iron (Fe^{3+} and Fe^{2+} ions) in basic solution. Subsequently, a small layer of silica around the MNPs was formed using sol–gel approach, which further prevented the agglomeration of the Fe_3O_4 nanoparticles. Subsequently, the amine (NH_2) functionalities were introduced onto the surface of SMNPs using 3-aminopropyl triethoxysilane (APTES). In order to enhance the number of NH_2 groups on the surface, biguanidine moiety was introduced. Finally, the obtained magnetic nanoparticles (NPs) were subjected to sulfonation using chlorosulfonic acid in order to obtain acidic catalyst ($NP@SO_3H$). Finally, the structure of the nanocatalyst was confirmed systematically by characterization using various modern sophisticated techniques such as FT-IR, PXRD, SEM, TEM, EDS, and VSM.

Fourier transform infrared spectroscopy (FT-IR)

The FT-IR spectra was recorded to affirm the various functional groups present in these nanocomposite. The FT-IR spectrum of Fe_3O_4 depicts an intense bands at 580 cm^{-1} due to Fe–O vibration and a broad band at 3360 cm^{-1}, which is attributed to the surface –OH groups (Fig. 3a).[44] Further, silica coating over Fe_3O_4 was established by the presence of characteristic peaks at 921 cm^{-1} and 1081 cm^{-1}, which are attributed to Si–O–Si asymmetric stretching vibrations (Fig. 3b). For ASMNPs the bands centred at 3284 cm^{-1} represents the asymmetric stretching vibrations of N–H groups[45] (Fig. 3c). Fig. 3d represents the FT-IR spectra of NPs. Further, the presence of sulfonyl moiety is asserted with 1188 and 994 cm^{-1} bands in FT-IR spectra (Fig. 3e).[46]

Powder X-ray diffraction (PXRD) analysis

To check purity and crystallographic structure of synthesized nanoparticles, powder XRD was carried out and represented in Fig. 4. Fig. 4a displayed Bragg peaks at 2θ = 30.3, 35.6, 43.3, 57.4, 62.9°, which are attributed to (2 2 0), (3 1 1), (4 0 0), (5 1 1), and (4 4 0) crystallographic faces of magnetite, respectively.[34] Similar peaks were obtained for $NP@SO_3H$ (Fig. 4b), which indicated the retention of crystalline magnetic core after silica coating and fabrication with various functional groups.

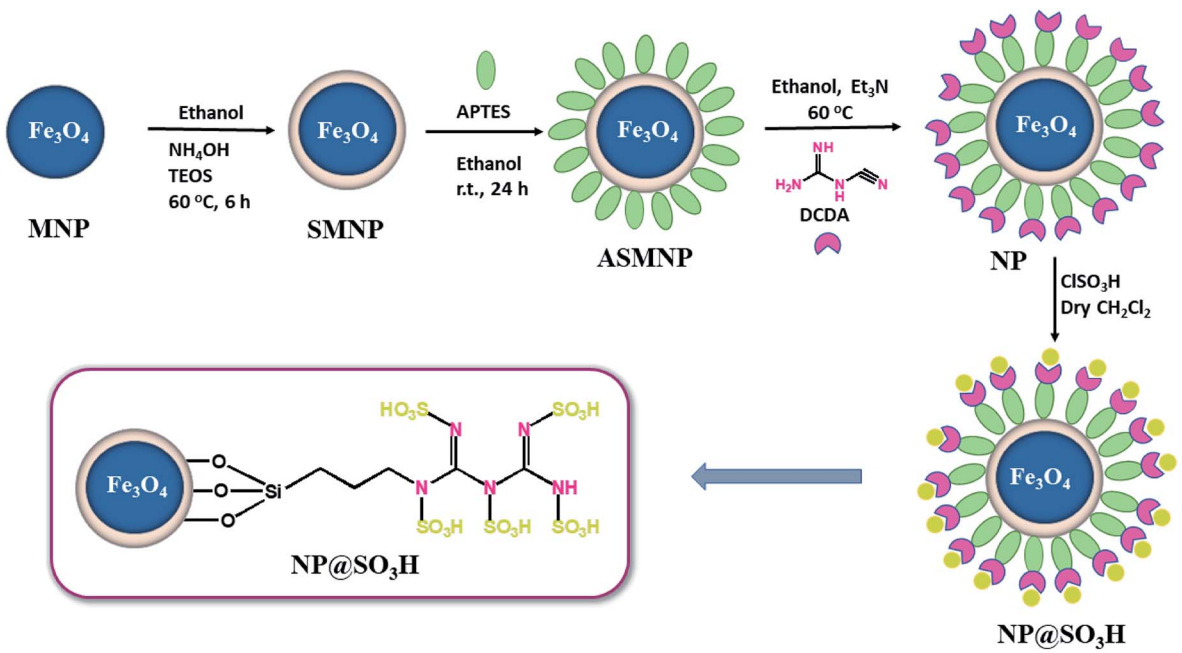

Scheme 1 Schematic illustration of formation of sulfonated magnetic nanoparticles ($NP@SO_3H$).

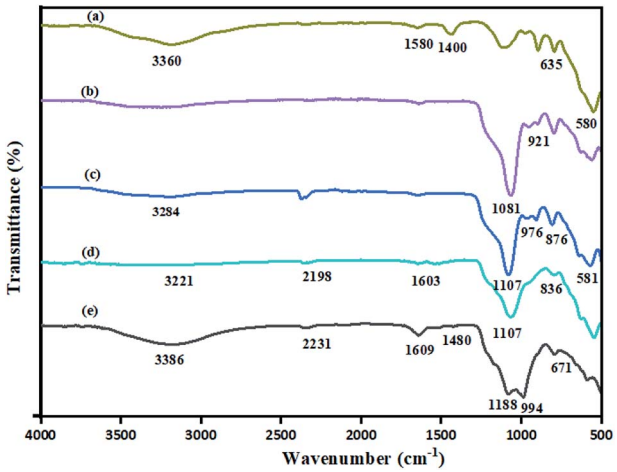

Fig. 3 FT-IR curves of (a) MNPs, (b) SMNPs, (c) ASMNPs, (d) NPs and (e) NP@SO_3H.

SEM TEM analysis

The size, shape and morphology aspects of the newer NP@SO_3H were analysed using TEM and SEM analysis (Fig. 5). TEM analysis reveals that the size of the nanocatalyst ranged from 34–50 nm. Moreover, the study reveals that the catalyst is made up with core shell structure having spherical morphology. However, the exact size of the particles was difficult to determine because the particles aggregate due to their paramagnetic nature. Further, it is evident from the SEM imaging, that the particles are roughly spherical in nature.

Further, to gain knowledge of stoichiometric distribution of elements in the synthesized NP@SO_3H nanocatalyst, EDX spectrum was collected. The collected EDX spectrum revealed the presence of expected constituent elements like iron, oxygen, silicon, sulphur and nitrogen in the sample (Fig. 6).

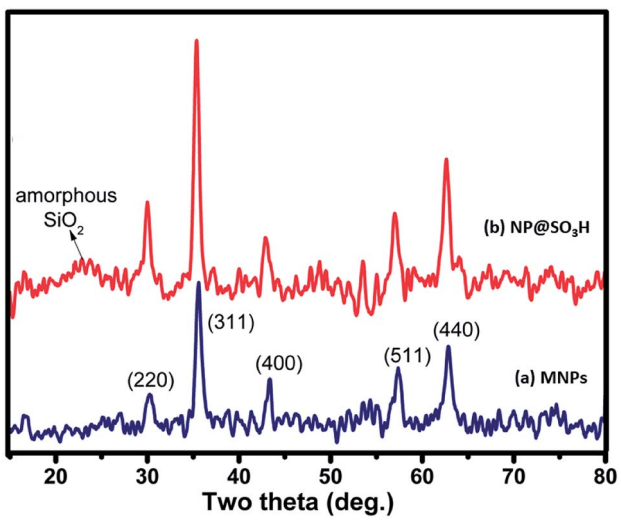

Fig. 4 PXRD patterns of (a) Fe_3O_4 (MNPs), (b) NP@SO_3H.

Vibrating sample magnetometric analysis (VSM)

Magnetization measurements of well dried magnetic nanoparticles were determined using vibration sample magnetometer (VSM) at room temperature in the external magnetic range of −10 000 to +10 000 Oe. The magnetic hysteresis curves suggested the super magnetic behaviour of these nanoparticles. It is evident from Fig. 7 that the MNPs, SMNPs, ASMNPs, NPs and NP@SO_3H showed a saturation magnetization value of 56, 43, 37, 28 and 21 emu g^{-1} respectively.

This decline in saturation magnetization was accredited to the existence of non-magnetic amorphous coatings of SiO_2 and functional groups over the surface of MNPs. Irrespective of the lower saturation magnetization (M_s) value than MNPs, NP@SO_3H can be separated smoothly from reaction mixture using an external magnet.

Evaluation of the catalytic activity of the NP@SO_3H for *N*-formylation of amines

After the successful characterization of the synthesized magnetic nanocatalyst (NP@SO_3H), its catalytic activity was explored for *N*-formylation of amines with formic acid under different reaction conditions (Table 1). The optimization of reaction conditions such as amount of catalyst, effect of solvents, temperature *etc.* were carried out using aniline (1 mmol) and formic acid (4.0 mmol) as model substrates. The reaction was carefully monitored by thin layer chromatography (TLC) for its completion manifested by the complete consumption of the aniline.

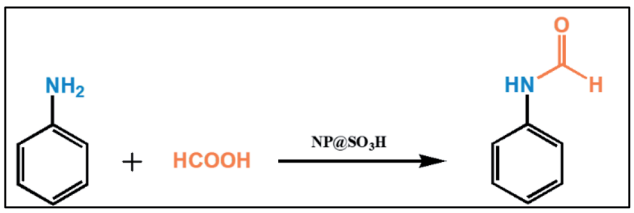

Firstly, we started our investigation by optimizing the amount of the catalyst. The amount of catalyst was varied from 0–20 mg (Table 1, entry 1–6) and it was observed 10 mg of NP@SO_3H is sufficient to carry out the reaction (Table 1, entry 4). When the amount of catalyst was reduced to 5 mg and increased up to 20 mg, the yield of product was found to be 64% and 95%, respectively. Thus, the optimum amount of catalyst was found 10 mg, as decrease in the catalyst amount resulted in decrease in the yield of the product (Table 1, entry 2 and 3) whereas an increase in the catalyst amount had no such significant effect on the percentage yield of product (Table 1, entry 5 and 6). Further, the yield of product was found to be maximum when ethanol was taken as solvent in comparison to CH_3CN, H_2O, THF and under the solvent free condition (Table 1, entry 4 and 7–10). The increase in yield can be attributed to better dispersion of magnetic NP@SO_3H nanoparticles in the ethanol. Further, ethanol being a green solvent maintains the spirit of green chemistry.

After optimizing the reaction conditions we examined the applicability of NP@SO_3H nanocatalyst for *N*-formylation of diverse aromatic amines using formic acid. As shown in Fig. 8, the reactions of all the substituted aromatic amines proceeded

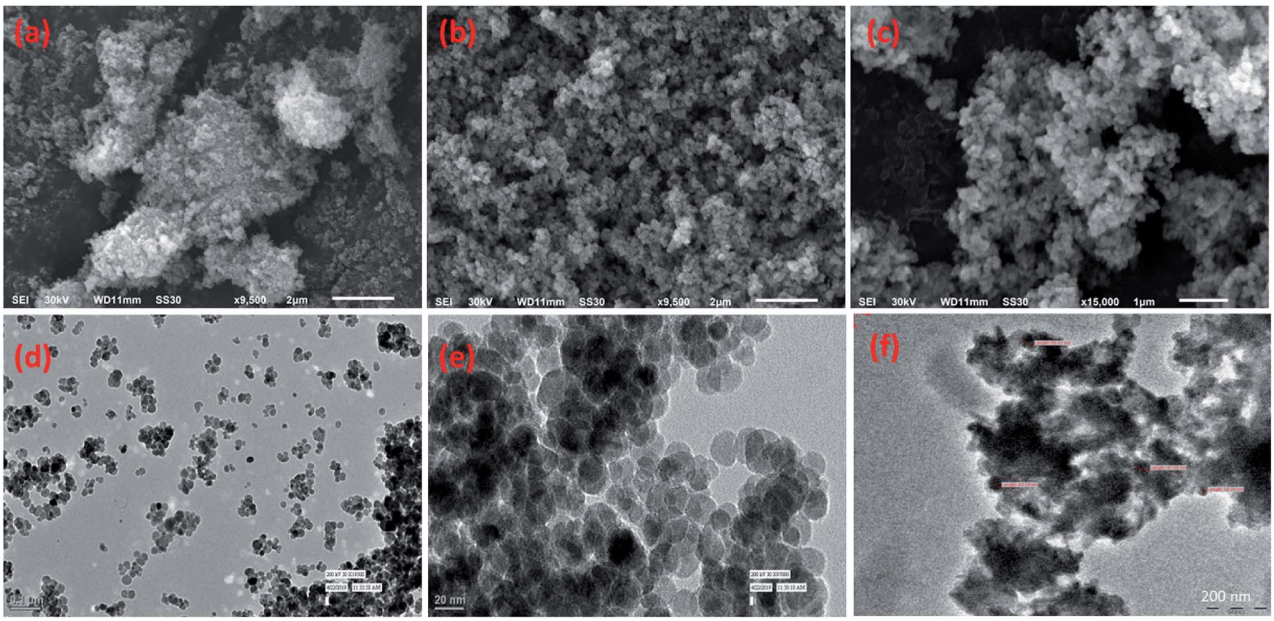

Fig. 5 SEM images of MNPs (a), SMNPs (b) SMNPs, (c) NP@SO_3H and TEM images of (d) MNPs, (e) SMNPs and (f) NP@SO_3H.

very smoothly and efficiently with no side products. However, the reaction was largely dependent on the substituent on the aromatic ring in terms of product yield. The anilines bearing an electron-donating group like methyl, methoxy, or hydroxyl proceeded more effectively than the reactions of anilines with an electron-withdrawing group such as chlorine, bromine (Fig. 8). Thus, NP@SO_3H showed admirable activity with diversified aniline substrates in a short reaction time (10 min) and with excellent yields (83–95%).

Proposed reaction mechanism

The role of nanocatalyst NP@SO_3H in the synthesis of formamide is shown in Fig. 9. Presumably, the mechanism of the reaction proceeds through activation of carbonyl group of formic acid *in situ* by the action of SO_3H group of nanocatalyst.[47,48] In the first step, the SO_3H proton of the nanocatalyst interacts with the oxygen atom of the carbonyl group of the formic acid, thereby increasing the electrophilic character of the carbonyl carbon probably through hydrogen bond formation. Then, the lone pair of electron on the nitrogen atom of aniline attack the cationic carbon of formic acid. Finally, dehydration of a water molecule leads to the formation of formamide, and the NP@SO_3H nanocatalyst is regenerated back and reused in subsequent catalytic cycles.

Reusability

The recovery or recyclability of catalyst is an important factor and determining factor for chemical industries. Therefore, the recovery and reusability of NP@SO_3H was investigated (Fig. 10). After the completion of reaction, the catalyst was separated by external magnet, washed with ethanol and dried at 60 °C in oven for 1 h, and reused under similar reaction condition. As shown in Fig. 10, our experiment showed that the catalyst can be reused at least six times without any significant loss of its

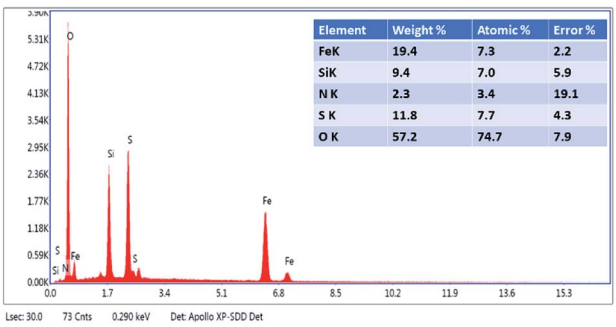

Fig. 6 EDX of NP@SO_3H.

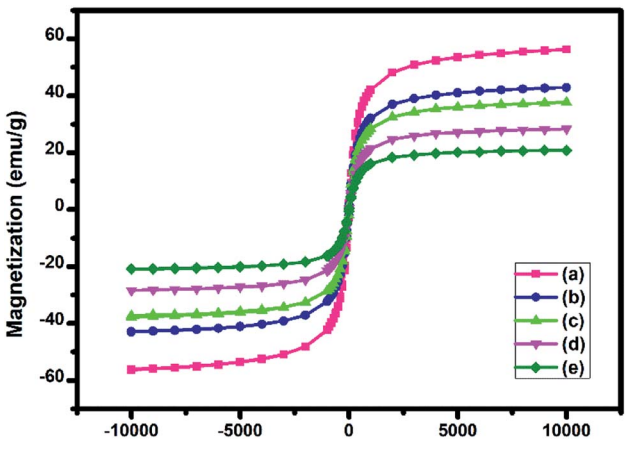

Fig. 7 Magnetization curves obtained using VSM for the (a) MNPs, (b) SMNPs, (c) ASMNPs, (d) NPs and (e) NP@SO_3H at room temperature.

catalytic activity. The results were further verified by FT-IR and powder XRD of reused catalyst obtained after 6 serial runs (Fig. S1 and S2 of ESI†), which demonstrated the intact of structure and morphology of the nanocatalyst. Thus, NP@SO_3H proved to be efficient catalyst giving high yields of product in shorter reaction times (10 min). In addition, the advantages of NP@SO_3H nanocatalyst are its ease of magnetic separation, recyclability and its very simple work-up.

Comparison with the literature precedents of *N*-formylation of amines using formic acid

Further, extensive literature survey divulges that various heterogeneous as well as homogeneous catalyst have been described for the *N*-formylation of amines using formic acid as oxidant (Table 2). However, the present solid acid catalyst was found to be superior to previously reported catalysts in terms of mild reaction conditions, yield of product, reaction time and

Table 1 Optimization of reaction conditions[a]

Entry	Catalyst[b]	Solvent	Temp/time[c]	Yield[d] (%)
1	0	EtOH	RT/30	NR
2	5	EtOH	RT/10	64
3	7	EtOH	RT/10	80
4	**10**	**EtOH**	**RT/10**	**95**
5	15	EtOH	RT/10	94
6	20	EtOH	RT/10	95
7	10	EtOH	70/10	83
7	10	CH_3CN	RT/10	60
8	10	THF	RT/10	65
9	10	H_2O	RT/10	53
10	10	Solvent free	RT/10	87

[a] Reaction conditions: aniline (1.0 mmol), formic acid (4.0 mmol), solvent (2 mL). [b] Catalyst (mg). [c] Temp (°C) and time (min). [d] % isolated yield.

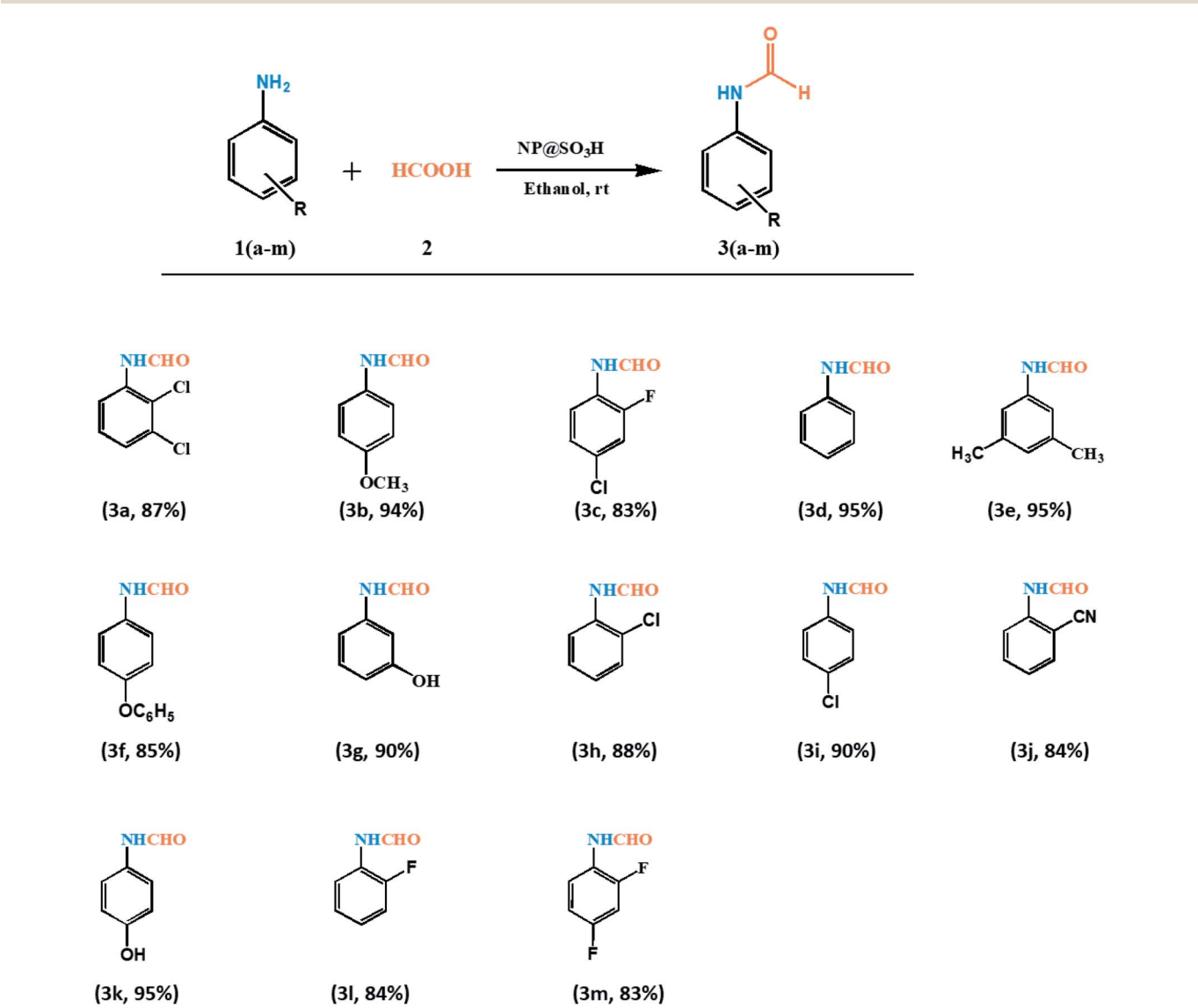

Fig. 8 List of synthesized compounds. Reaction conditions: aniline (1 mmol), formic acid (4.0 mmol), ethanol (2 mL), catalyst (10 mg), rt, 10 min.

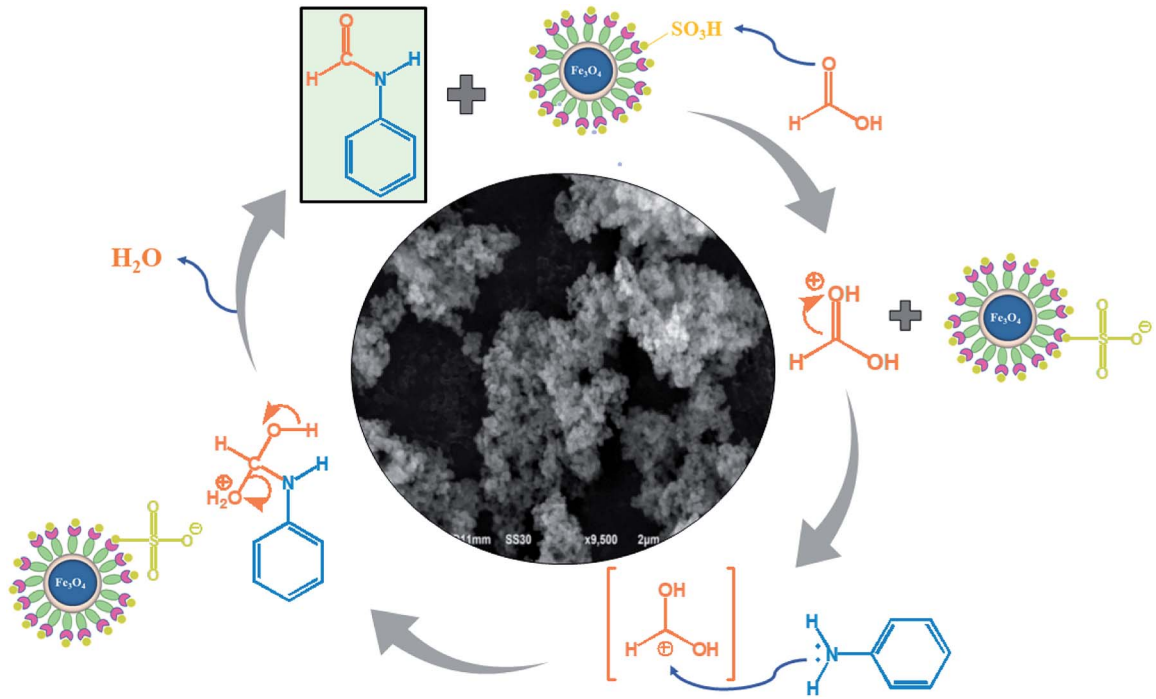

Fig. 9 Plausible mechanism for the *N*-formylation of amines catalysed by NP@SO_3H.

exceptional recyclability of the catalyst (Table 2). This outstanding catalytic performed can be credited to the presence of large number of catalytic sites.

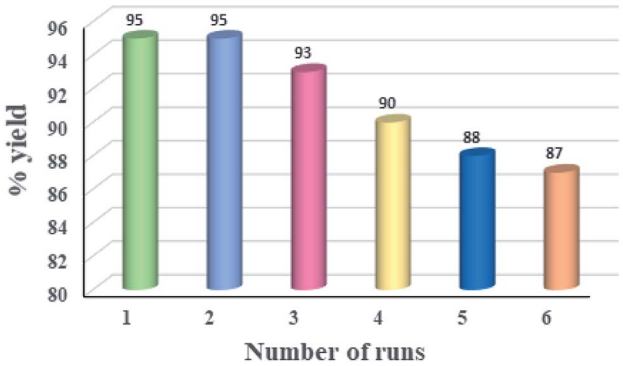

Fig. 10 Recyclability of the NP@SO_3H nanocatalyst in the *N*-formylation of aniline with formic acid.

Table 2 Previously reported catalyst for *N*-formylation of amines using formic acid as formylating agent

S. No.	Catalyst	Solvent	*T* (°C)	Time (min)	Ref.
1	DES/SBA-15	Solvent-free	r.t.	40–120	47
2	[PVP-SO_3H] HSO_4	Solvent-free	60	2–20	48
3	CuO/HZSM-5	Solvent-free	r.t.	10–100	49
4	Nano-Al_2O_3	Solvent-free	40–70	5–300	50
5	Co_3O_4 NPs	Solvent-free	40	4–20	51
6	Fe_3O_4@phendiol@Co	Solvent-free	r.t.	8–200	52
7	$CoFe_2O_4$@SiO_2-PTA	Solvent-free	r.t.	25–60	53
8	γ-Fe_2O_3@HAP-SO_3H	Solvent-free	r.t.	15–60	54
9	NP@SO_3H	EtOH	r.t.	10	P.W.

Conclusions

In the present study, NP@SO_3H heterogeneous magnetic nanocatalyst was successfully synthesized, characterized and was used perform *N*-formylation of primary aromatic amines using formic acid at room temperature within 10 minutes. The notable features of prepared heterogeneous acid catalyst are ease of recovered by using an external magnetic force. Further, it could be reused up to six catalytic cycles without any significant loss in catalytic activity. In addition to the simplistic catalytic recovery and excellent recycling efficiency, the use of inexpensive materials makes this protocol economically practicable and superior to earlier established protocols. Some of the other fascinating features that adds to the effectiveness of present work are mild reaction conditions, use of non-toxic chemicals, shorter reaction period, simple workup procedure and broad substrate scope. Thus, present catalytic system will encourage green and sustainable organic synthesis by opening up new opportunities for the large scale synthesis of several other industrially significant products.

Conflicts of interest

Authors declares no conflicts of interest.

Acknowledgements

JKY and AA are thankful to Banaras Hindu University, Varanasi, India, for the financial support. PY is thankful to UGC, New Delhi for financial support. Authors are thankful to, USIC-CIF University of Delhi, Delhi, India for providing instrumentation facilities. The authors would also like to acknowledge SAIF-

AIIMS, New Delhi, India for TEM analysis. SKA is also thankful to the SERB (F/9974/20-17) and University of Delhi for generous financial support.

References

1 X. F. Li, X. G. Zhang, F. Chen and X. H. Zhang, *J. Org. Chem.*, 2018, **83**, 12815–12821.
2 I. M. Dowine, M. J. Earle, H. Heaney and K. F. Shuhaibar, *Tetrahedron*, 1993, **49**, 4015–4034.
3 K. P. Dhake, P. J. Tambade, R. S. Singhal and B. M. Bhanage, *Green Chem. Lett. Rev.*, 2011, **4**, 151–157.
4 S. L. Yedage, D. S. Dsilva and B. M. Bhanage, *RSC Adv.*, 2015, **5**, 80441–80449.
5 R. B. Sonawane, N. K. Rasal and S. V. Jagtap, *Org. Lett.*, 2017, **19**, 2078–2081.
6 S. Kobayashi and K. Nishio, *J. Org. Chem.*, 1994, **59**, 6620–6628.
7 K. Shu, Y. Masaru and H. Iwao, *Chem. Lett.*, 1996, **25**, 407–408.
8 B. Das, M. Krishnaiah, P. Balasubramanyam, B. Veeranjaneyulu and D. N. Kumar, *Tetrahedron Lett.*, 2008, **49**, 2225–2227.
9 P. Ju, J. Chen, A. Chen, L. Chen and Y. Yu, *ACS Sustainable Chem. Eng.*, 2017, **5**, 2516–2528.
10 M. Waki and J. Meinhofer, *J. Org. Chem.*, 1977, **42**, 2019–2020.
11 F. M. F. Chen and L. N. Benoiton, *Synthesis*, 1979, **9**, 709–710.
12 S. H. Jung, J. H. Ahn, S. K. Park and J. K. Choi, *Bull. Korean Chem. Soc.*, 2002, **23**, 149–150.
13 R. B. Sonawane, N. K. Rasal and S. V. Jagtap, *Org. Lett.*, 2017, **19**, 2078–2081.
14 P. Strazzolini, A. G. Giumanini and S. Cauci, *Tetrahedron*, 1990, **46**, 1081–1118.
15 P. G. Reddy, G. D. K. Kumar and S. Baskaran, *Tetrahedron Lett.*, 2000, **41**, 9149–9151.
16 F. F. Blicke and C. J. Lu, *J. Am. Chem. Soc.*, 1952, **74**, 3933–3934.
17 J. Deutsch, R. Eckelt, A. Kockritz and A. Martin, *Tetrahedron*, 2009, **65**, 10365–10369.
18 N. Shah, E. Gravel, D. V. Jawale, E. Doris and I. N. N. Namboothiri, *ChemCatChem*, 2014, **6**, 2201–2205.
19 L. B. Figueroa, A. O. Porras and D. G. Sanchez, *J. Org. Chem.*, 2014, **79**, 4544–4552.
20 D. W. Gu and X. X. Guo, *Tetrahedron*, 2015, **71**, 9117–9122.
21 A. C. shekhar, A. R. kumar, G. Sathaiah, V. L. paul, M. Sridhar and P. S. rao, *Tetrahedron Lett.*, 2009, **50**, 7099–7101.
22 M. H. Sarvari and H. Sharghi, *J. Org. Chem.*, 2006, **71**, 6652–6654.
23 N. Shah, E. Gravel, D. V. Jawale, E. Doris and I. N. N. Namboothiri, *ChemCatChem*, 2014, **6**, 2201–2205.
24 J. G. Kim and D. O. Jang, *Synlett*, 2010, **8**, 1231–1234.
25 S. M. Sajadi, M. Maham and A. Rezaei, *Lett. Org. Chem.*, 2014, **11**, 49–54.
26 Y. J. Kim, J. W. Lee, H. J. Lee, S. Zhang, J. S. Lee, M. Cheong and H. S. Kim, *Appl. Catal., A*, 2015, **506**, 126–133.
27 Z. Chen, R. Fu, W. Chai, H. Zheng, L. Sun, Q. Lu and R. Yuan, *Tetrahedron*, 2014, **70**, 2237–2245.
28 M. Nirmala, G. Prakash, P. Viswanathamurthi and J. G. Malecki, *J. Mol. Catal. A: Chem.*, 2015, **403**, 15–26.
29 B. Karami, M. Farahi and F. Pam, *Tetrahedron Lett.*, 2014, **55**, 6292–6296.
30 S. K. Rasheed, D. N. Rao, A. S. Reddy, R. Shankar and P. Das, *RSC Adv.*, 2015, **5**, 10567–10574.
31 S. P. Pathare, R. V. Sawant and K. G. Akamanchi, *Tetrahedron Lett.*, 2012, **53**, 3259–3263.
32 M. Rahman, D. Kundu, A. Hajra and A. Majee, *Tetrahedron Lett.*, 2010, **51**, 2896–2899.
33 S. Joseph, P. Das, B. Srivastava, H. Nizar and M. Prasad, *Tetrahedron Lett.*, 2013, **54**, 929–931.
34 P. Singh, P. Yadav, A. Mishra and S. K. Awasthi, *ACS Omega*, 2020, **5**, 4223–4232.
35 S. Fortun and A. R. Schmitzer, *ACS Omega*, 2018, **3**, 1889–1896.
36 M. Beygzadeh, A. Alizadeh, M. M. Khodaei and D. Kordestani, *Catal. Commun.*, 2013, **32**, 86–91.
37 K. Nakajima and M. Hara, *ACS Catal.*, 2012, **2**, 1296–1304.
38 N. Koukabi, E. Kolvari, M. A. Zolfigol, A. Khazaei, B. S Shaghasemi and B. Fasahati, *Adv. Synth. Catal.*, 2012, **354**, 2001–2008.
39 A. Rahmatpour, *Catal. Lett.*, 2012, **142**, 1505–1511.
40 *Hazards in the chemical laboratory*, ed. S. G. Luxon, Royal Society of Chemistry, Cambridge, 1992, p. 302.
41 H. Singh, J. K. Rajput and P. Arora, *RSC Adv.*, 2016, **6**, 84658–84671.
42 Z. Wang, j. Xie, M. Shen, S. Nie and M. Xie, *Trends Food Sci. Technol.*, 2018, **74**, 147–157.
43 Z. G. Wang and M. Lu, *RSC Adv.*, 2014, **4**, 1234–1240.
44 C. Garkoti, J. Shabir and S. Mozumdar, *New J. Chem.*, 2017, **41**, 9291–9298.
45 M. Z. Kassaee, H. Masrouri and F. Movahedi, *Appl. Catal., A*, 2011, **395**, 28–33.
46 D. Azarifar, O. Badalkhani and Y. Abbasi, *J. Sulfur Chem.*, 2016, **37**, 656–673.
47 N. Azizi, M. Edrisi and F. Abbasi, *Appl. Organomet. Chem.*, 2018, **32**, 3901.
48 F. Pakpour-Roudsari, M. Seddighi, F. Shirini and H. Tajik, *ChemistrySelect*, 2019, **4**, 6382–6389.
49 M. Tajbakhsh, H. Alinezhad, M. Nasrollahzadeh and T. A. Kamali, *J. Colloid Interface Sci.*, 2016, **471**, 37–47.
50 V. K. Das, R. R. Devi, P. K. Raul and A. J. Thakur, *Green Chem.*, 2012, **14**, 847–854.
51 A. P. Marjani, S. A. Hosseini, Z. Shokri and N. Maleki, *Res. Chem. Intermed.*, 2017, **43**, 413–422.
52 D. Habibi, S. Heydari and M. Afsharfarnia, *Appl. Organomet. Chem.*, 2017, **31**, 3874.
53 M. Kooti and E. Nasiri, *J. Mol. Catal. A: Chem.*, 2015, **406**, 168–177.
54 L. Ma'mani, M. Sheykhan, A. Heydari, M. Faraji and Y. Yamini, *Appl. Catal., A*, 2010, **377**, 64–69.

